

United States
Department of
Agriculture

Forest Service

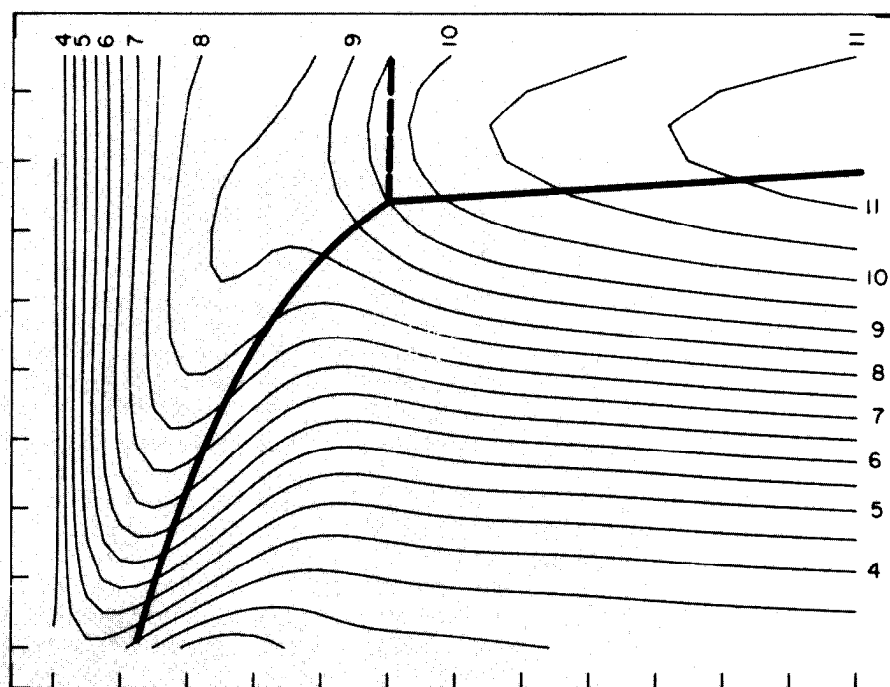
Forest
Products
Laboratory

Research
Paper
FPL 401



Effect of Paperboard Stress-Strain Characteristics on Strength of Singlewall Corrugated Fiberboard:

A Theoretical Approach



Abstract

The stress-strain relationship for paperboard loaded in edgewise compression relates to the strength of singlewall corrugated containers. This relationship can be approximated from the paperboard characteristics of stress measured at the maximum load and the initial modulus of elasticity. Based on typical characteristics for both linerboard and corrugating medium material a design matrix is constructed for a factorial analysis. Using a computer, various stress-strain relationships are paired together like they might be on the corrugator, and the theoretical effects of the stress-strain characteristics are investigated. Computer drawn design curves show how these linerboard and medium characteristics affect combined board edgewise compressive strength and box top-to-bottom compressive strength. The interaction between the stress-strain characteristics and paperboard thickness is used to suggest new criteria for evaluating paperboard.

United States
Department of
Agriculture

Forest Service

Forest
Products
Laboratory¹

Research
Paper
FPL 401

July 1981

Effect of Paperboard Stress-Strain Characteristics on Strength of Singlewall Corrugated Fiberboard: A Theoretical Approach

By
THOMAS J. URBANIK, Engineer

Introduction

There are increasing demands on corrugated containers to perform successfully in the service environments. As the container's environment is better defined, it becomes more rational to evaluate the container based on end use performance. Design criteria that relate the corrugated components to the container's performance in say, the warehouse environment, are likewise a more rational evaluation of paperboard. This report was written to characterize paperboard and then relate it to the container's important performance requirement of short term top-to-bottom compressive strength. It is limited to balanced singlewall under ideal test conditions.

Measuring container compressive strength is probably the most accurate evaluation of how well it will perform in the warehouse. Full-scale container testing is not always practical and thus engineering models have been devised that relate the components' behavior to box strength. The model developed by McKee, Gander, and Wachuta (7)² relates certain box and corrugated board parameters, such as edgewise compressive strength, bending stiffness, and box perimeter, to container strength. Based on the alternate approaches to combining various paperboards and maximizing box strength, this model does not adequately explain the paperboards' contribution to box compressive strength.

Koning (4) expanded on McKee, *et al.*'s formula to examine the effects of linerboard characteristics on container strength. Though good correlation was obtained between theoretical and experimental values (5), extending the solution process which relied on an approach by Moody (8) is inefficient for investigating the large number of possible combinations of paperboard.

Johnson, Urbanik, and Denniston (3) devised an efficient computer model that predicts the edgewise compressive strength of singlewall from the compression stress-strain relationships for both facing and medium material in the cross-machine direction (CMD) and the structural configuration of the board (fig. 1). They used it to study the effect of combining different thicknesses of linerboards and corrugating mediums on the edgewise compressive strength of A-flute corrugated. The results show how to balance facing and corrugating medium thicknesses to minimize total fiber weight and maximize edgewise compressive strength based on one characteristic pair of paperboard stress-strain curves. This previous research thus evaluated paperboard based on thickness but treated just one set of CMD stress-strain properties.

The purpose of this report is to extend the work by Johnson, *et al.*, and quantify how corrugated fiberboard changes strength due to differences in linerboard and corrugating medium stress-strain curves, and the interactions with thickness. To do this it was necessary to numerically characterize stress-strain curves, thus making it possible to efficiently analyze different curves. Then using experimental results to provide typical curves, numerical values were calculated using

¹ Maintained at Madison, Wis., in cooperation with the University of Wisconsin.

² Italicized numbers in parentheses refer to literature cited at end of report.

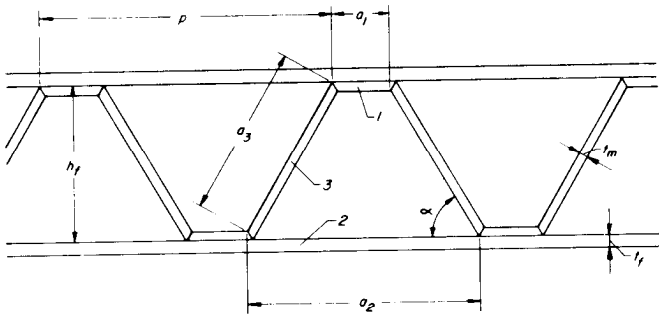


Figure 1.—Cross sectional model of singlewall corrugated fiberboard. (M 149 722)

a 2-parameter stress-strain model, and the resulting values used in a 2^4 factorial experiment to determine the effects of these different paperboards on A-flute corrugated strength. Results are presented with computerized plots, and these plots facilitate strength calculations for arbitrary theoretical stress-strain curves. An additional benefit from the plots is that they provide theoretical information about the buckling and compression behavior of corrugated fiberboard and explain how paperboard stress-strain characteristics interact with thickness to initiate failure in either the facing or medium component, thus suggesting new criteria for evaluating paperboard. This report also examines the effects on box top-to-bottom compressive strength as compared with those related to edgewise compressive strength.

The computer program developed in (3) is used here to enable over 10,000 computations to be made. Member dimensions for the figure 1 structure are calculated from the paperboard thicknesses and flute profile. Details are given in the appendix.

Characterizing the Compression Stress-Strain Curve

Stress-Strain Model

The computer program in (3) predicts edgewise compressive strength from certain fiberboard properties. Having the linerboard thickness, corrugating medium thickness, flutes per foot, flute height, and take-up-factor determines the widths of the paperboard elements between flute tips in figure 1. Then the buckling mode of failure of these elements is analyzed from their widths and their CMD stress-strain properties which are entered to the program by parameters to a stress-strain model characterizing each component. To check for a compression mode of failure in an element, the ultimate stress (σ_u) is also entered for each component. Thus for input values to the 2^4 factorial experiment it was necessary to numerically quantify the paperboard stress-strain curve so both buckling and compression modes could be investigated; in essence, provide experimental variables (factors) that give the continuous stress-strain curve shape and also yield σ_u .

Numerous investigators have researched the effects of various papermaking variables on the elastic modulus

and compressive strength of paper (1, 6, 9, 11). It seemed reasonable to numerically quantify stress-strain curves with the familiar characteristics of the initial modulus of elasticity (MOE) and σ_u .

To obtain the relations between σ_u and MOE and the stress-strain curve, this report characterizes the curve with a special form of the stress-strain model reported in (3) having 2 instead of 3 parameters and then relates σ_u and MOE to these parameters. The model is

$$\sigma(\epsilon) = C_1 \tanh(C_2\epsilon/C_1) \quad (1)$$

where σ is the predicted stress at a strain ϵ ; C_1 is a horizontal asymptote that σ approaches for very large ϵ ; C_2 is the initial slope of the curve. Since MOE is the derivative of σ relative to ϵ evaluated at zero,

$$\sigma'(\epsilon) = C_2/\cosh^2(C_2\epsilon/C_1) \quad (2-a)$$

and at $\epsilon = 0$

$$\sigma'(0) = C_2 = \text{MOE} \quad (2-b)$$

Thus having a characteristic MOE automatically gives C_2 . To automatically determine C_1 from the characteristic parameters the correlation f between C_1 and σ_u , where

$$C_1 = f(\sigma_u) \quad (3)$$

was determined for a specific set of data and used. Using σ_u and MOE as experimental variables depicting each component, and solving eqs. (2-b, 3), parameters C_1 , C_2 , and σ_u for each component were thus entered to the computer program to characterize the stress-strain behavior and analyze for buckling or compression failure in the fiberboard structure.

Experimental Check of Characterization

With a method to numerically characterize stress-strain curves in terms of σ_u and MOE, it was necessary to determine some reasonable values for use in the factorial design and check the accuracy of the characterization. To do this, 13 linerboards and 9 corrugating mediums, with replicates, were tested for edgewise compression in the cross-machine direction. The paperboards were constrained against buckling in a support fixture described by Jackson (2). Nominal basis weights ranged from 26 through 90 pounds per 1,000 square feet. Experimentally determined weights and effective thicknesses measured, using the Forest Products Laboratory (FPL) stylus apparatus (10), are given in table 1. A linear regression of the table 1 data gives the basis weight W and thickness t relationship, assuming equal slopes, as

$$W_l \text{ (lb/1,000 ft}^2\text{)} = 2.224 + 3,562 t_l \text{ (in.)} \quad (4-a)$$

$$W_{cm} \text{ (lb/1,000 ft}^2\text{)} = - 4.410 + 3,562 t_{cm} \text{ (in.)} \quad (4-b)$$

for the linerboard and corrugating medium respectively (fig. 2).

All materials were preconditioned at less than 35 percent relative humidity (RH) and then conditioned at 73°F and 50 percent RH prior to testing at this same condition. The load was applied at a constant rate of deformation and recorded with a digital oscilloscope. The compression machine speed produced a strain rate in the paperboard of 0.01504 in./in./min. The experimental load deformation curves were converted into stress-strain relationships. Stress is defined as the applied load per original cross sectional area based on effective thickness, and strain, as the deformation per undeformed specimen gage length. The resulting stress-strain relationships are shown by solid line curves in figure 3.

To determine the suitability of using $C_1 = f(\sigma_u)$ the best estimate of C_1 was obtained by fitting eq. (1) to the data of each curve with the nonlinear regression

routine NREG (12). These best estimates of C_1 are compared with the C_1 values based on $C_1 = f(\sigma_u)$ and are given in table 1. A regression analysis to determine the relationship between C_1 and σ_u is as follows:

$$C_1 = 1523. + 1.028 \cdot 10^{-7} \sigma_u^3 (\text{lb/in.}^2) \quad (5-a)$$

$$C_1 = 44.91 + 1.120 \sigma_u (\text{lb/in.}^2) \quad (5-b)$$

Eq. (5-a) is used for linerboard and (5-b) for corrugating medium. Table 1 gives the predictions for C_1 as calculated from eqs. (5-a,-b) and compares them with the best estimates obtained from the eq. (1) curve fit. The correlation coefficient r equals 0.9433. Figure 4 shows the plot of C_1 versus σ_u , and the regression curves.

When eq. (1) is fit to the stress-strain data, the initial modulus, MOE, is determined from parameter C_2 ; in

Table 1.--Data and predictions

Specimen number	Effective thickness (t)	Basis weight (W)	Ultimate stress (s_u)	Eq. (1) coefficients			
				C_1			C_2 Initial modulus of elasticity
				Best estimate	$f(s_u)$	Difference	
	<u>0.001 in.</u>	<u>Lb/1,000 ft²</u>	<u>Lb/in.²</u>	<u>Lb/in.²</u>	<u>Lb/in.²</u>	<u>Pct</u>	<u>Lb/in.²</u>
CORRUGATING MEDIUM							
1	8.47	26.12	1,316	1,576	1,518	3.65	248,700
2	8.47	26.12	1,441	1,704	1,658	2.68	265,400
3	8.50	26.10	1,577	1,733	1,811	- 4.48	336,200
4	8.50	26.10	1,503	1,711	1,728	- .98	370,200
5	8.53	26.88	1,543	1,815	1,773	2.34	345,300
6	8.53	26.88	1,644	2,002	1,886	5.81	335,000
7	8.53	28.16	1,367	1,586	1,576	.66	233,200
8	8.53	28.16	1,429	1,618	1,645	- 1.66	235,500
9	8.73	26.22	1,421	1,787	2,046	- 14.51	296,100
10	8.73	26.22	1,512	1,769	1,738	1.76	369,400
11	8.97	26.79	1,537	1,704	1,766	-3.63	335,000
12	8.97	26.79	1,537	1,743	1,766	-1.31	324,900
13	9.00	26.87	1,682	1,891	1,928	-1.97	294,600
14	9.00	26.87	1,361	1,575	1,569	.39	273,900
15	9.07	27.24	1,227	1,424	1,419	.37	252,000
16	9.07	27.24	1,126	1,293	1,306	- .98	245,500
17	9.17	27.24	1,380	1,532	1,590	- 3.97	253,900
18	9.17	27.24	<u>1,171</u>	1,355	1,356	- .08	<u>215,700</u>
Average			1,432				290,600
Standard deviation			154.1				49,860

Table 1.–Data and predictions (continued)

Specimen number	Effective thickness (t)	Basis weight (W)	Ultimate stress (s _u)	Eq. (1) coefficients			
				C ₁			C ₂ Initial modulus of elasticity
				Best estimate	f(s _u)	Difference	
<u>0.001 in.</u>	<u>Lb/1,000 ft²</u>	<u>Lb/in.²</u>	<u>Lb/in.²</u>	<u>Lb/in.²</u>	<u>Pct</u>	<u>Lb/in.²</u>	
LINERBOARD							
19	10.87	41.63	1,581	1,974	1,929	2.27	323,500
20	10.87	41.63	1,946	2,239	2,281	.54	328,400
21	11.30	42.27	1,659	2,166	1,992	8.02	335,600
22	11.30	42.27	1,365	1,822	1,784	2.07	316,900
23	11.43	41.86	1,687	2,087	2,017	3.38	323,100
24	11.43	41.86	1,900	2,285	2,228	2.49	344,600
25	12.00	44.72	1,545	1,850	1,902	- 2.81	261,700
26	12.00	44.72	1,707	2,037	2,034	.13	285,800
27	12.35	44.51	1,694	1,922	2,023	- 5.24	298,200
28	12.35	44.51	1,569	1,914	1,920	- .31	277,600
29	18.05	71.28	2,005	2,417	2,352	2.70	307,300
30	18.05	71.28	1,819	2,153	2,142	.52	288,900
31	19.90	67.65	1,583	1,893	1,931	- 1.99	246,500
32	19.90	67.65	1,618	1,923	1,958	- 1.84	242,300
33	23.37	92.49	1,954	2,272	2,290	- .79	299,000
34	23.37	92.49	2,058	2,416	2,419	- .13	318,800
35	24.20	90.48	1,977	2,388	2,317	2.95	301,500
36	24.20	90.48	2,050	2,242	2,409	- 7.44	298,300
37	25.07	96.43	1,895	2,364	2,223	5.98	301,800
38	25.07	96.43	2,108	2,558	2,486	2.81	302,200
39	25.10	87.09	1,869	2,010	2,194	- 9.16	257,200
40	25.10	87.09	1,510	1,838	1,877	- 2.11	263,800
41	25.10	87.09	1,785	2,032	2,108	- 3.72	272,100
42	25.20	93.32	1,704	2,370	2,891	- 22.00	261,600
43	25.20	93.32	1,990	2,326	2,333	- .31	279,100
44	27.40	94.62	1,923	2,199	2,254	- 2.51	252,500
45	27.40	94.62	<u>1,879</u>	2,227	2,205	.99	<u>273,100</u>
Average			1,792				291,200
Standard deviation			196.5				28,450

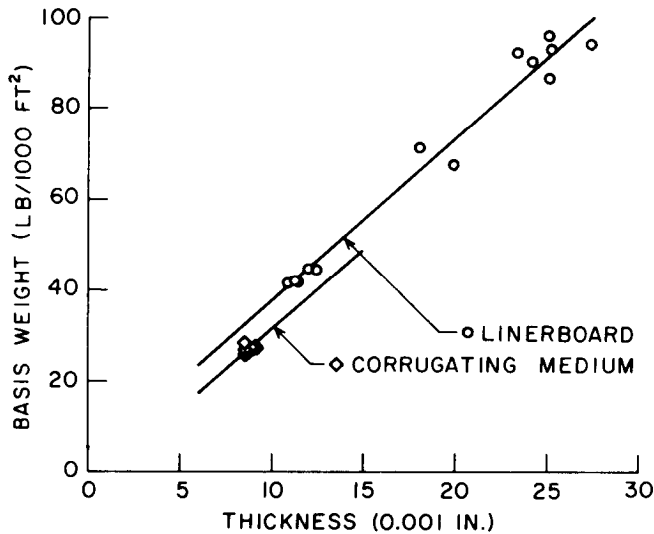


Figure 2.—Basis weight versus thickness observed in table 1 data. (M 148 287)

essence, $C_2 = MOE$. From the σ_u and MOE for each experimental curve and eqs. (1, 5-a, 5-b), the predicted stress-strain curve is shown by a superimposed dashed line in figure 3. Except for linerboards 36 and 39 the characterization is very good. Based on the paperboards tested for this study, values of σ_u and MOE could be used to accurately represent the continuous shape of the stress-strain curve of paperboard loaded in edgewise compression.

Factorial Development

To produce a set of theoretical stress-strain curves and evaluate the effects of different curves and the interactions between facings and corrugating medium the data in table 1 were used and a 2^4 factorial experiment

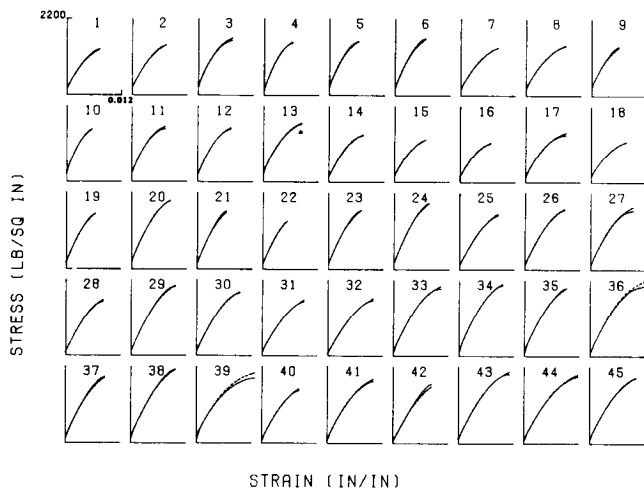


Figure 3.—Stress-strain curves produced by load-deformation data (solid lines) and predicted curves (dashed lines) determined from the s_u and MOE in the data. Corrugating medium (1-18) and linerboard (19-45). (M 148 820)

was designed. The four factors and their average values used in the design were linerboard $\sigma_u = 1,792$, linerboard MOE = 291,200, corrugating medium $\sigma_u = 1,432$, and corrugating medium MOE = 290,600. Using these averages, a high and a low value for each factor was determined for input to a factorial analysis by adding or subtracting 12.5 percent from each average. Then by permuting the different combinations of high and low values and using the characterization discussed in the previous section there were obtained four theoretical linerboard curves, numbered 1-4, and four theoretical medium curves, numbered 5-8. The levels of σ_u and MOE and the eq. (1) coefficients for these curves are given in table 2. These representative linerboard and medium curves were paired together like they might be in combining on the corrugator and are plotted in figure 5.

Table 3 outlines the 2^4 factorial design. The design matrix factors are σ_u and MOE for the facings, and σ_u , and MOE for the medium. These various combinations of high and low values thus fix the stress-strain behaviors (i.e., C_1 , C_2 , and σ_u) for both components and provide the input to edgewise compressive strength calculations for each of 16 runs. The stress-strain pairs can be identified from the run numbers in figure 5.

Results of Factorial Analysis

Effects of Stress-Strain Characteristics on 42-26-42 A-Flute

Using this numerically produced data an example is given that examines the effects of the stress-strain characteristics on A-flute edgewise compressive strength for one common combination of components.

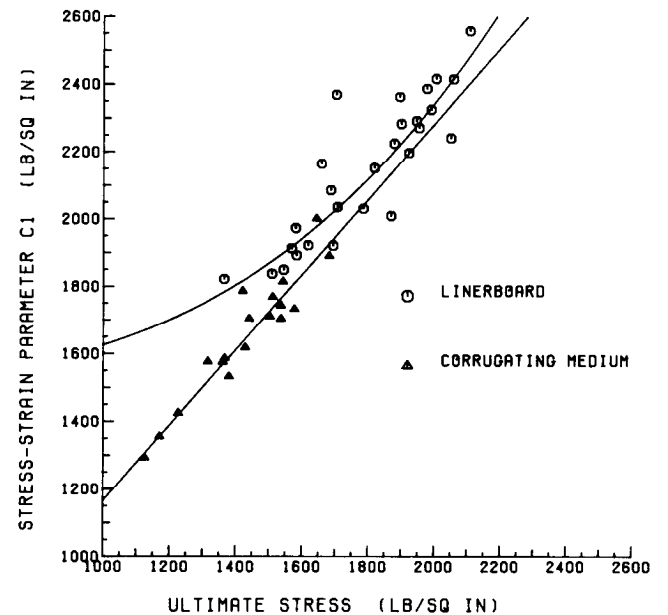


Figure 4.—Relation between stress-strain parameter C_1 and the ultimate stress σ_u used in this study. (M 148 818)

Table 2.—Typical stress-strain characteristics and parameters to representative stress-strain curves

Curve No.	Ultimate stress (s_u)	Initial Modulus of Elasticity (C_2)	C_1
	Lb/in. ²	Lb/in. ²	
LINERBOARD			
1	1,568	254,800	1,919
2	2,016	254,800	2,365
3	1,568	327,600	1,919
4	2,016	327,600	2,365
CORRUGATING MEDIUM			
5	1,253	254,300	1,448
6	1,611	254,300	1,849
7	1,253	326,900	1,448
8	1,611	326,900	1,849

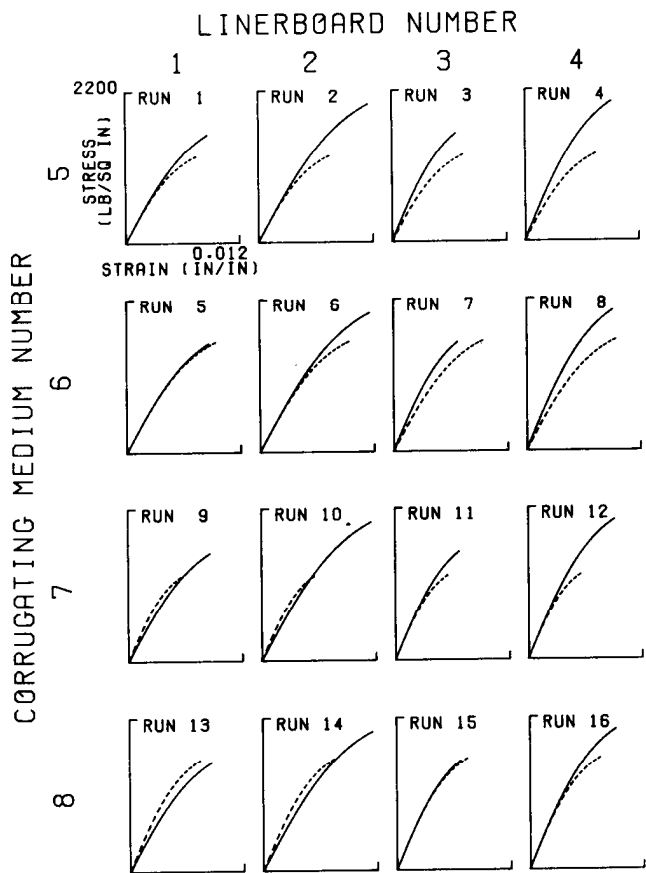


Figure 5.—Stress-strain relationships for linerboard (solid lines, 1-4) and corrugating medium (dashed lines, 5-8) paired together like they might be on the corrugator for 16 runs in a factorial analysis. The specific shapes are derived from data to cover the range of empirical observations. (M 148 817)

Consider a nominal 42-26-42 A-flute board with 36 flutes per foot, 0.18-inch flute height, and a 1.56 takeup factor. Based on eqs. (4-a,-b) the facings and medium are respectively 0.0112- and 0.00854-inch-thick. Assign the stress-strain properties to the components for each of the 16 runs from table 3. These combinations are shown in figure 5. Then the flute profile, component thicknesses, and paperboard stress-strain properties provide all the information to predict edgewise compressive strength according to the algorithm in (3). The results of the calculations are given in table 3 and they show that for this set of stress-strain curves the theoretical edgewise compressive strength for the 42-26-42, A-flute board varies from 40.65 to 55.31 lb/in. depending on how the stress-strain curves are paired together. An average strength for all the runs is predicted at 47.41 lb/in.

The predicted effects of the stress-strain characteristics, i.e., σ_u and MOE for both linerboard and corrugating medium, were measured by analyzing the numerically produced data by the usual methods applied to factorials, and are reported in table 4 as a percentage of the average edgewise compressive strength. For example, increasing the linerboard MOE 25 percent, i.e., from 12.5 percent below to 12.5 percent above the average of 291,200 lb/in., and holding all other factors fixed increases the edgewise compressive strength by 8.749 percent above the average of 47.41 lb/in. The predicted effects of the other factors and their interactions are also given relative to the average edgewise compressive strength. The significance of the interactions among various stress-strain characteristics is discussed in a following section "Relationship Between Mechanism of Failure and Optimum Design."

interaction of Stress-Strain Characteristics with Components' Thicknesses

It was of interest to repeat the analysis on other designs such as 69-33-69 A-flute and then check to see if the predicted effects are the same as for the 42-26-42 A-flute. However, the ever increasing amount of data for more than a few select designs made the tabular reporting of results impractical. The results from factorial analyses on other linerboard-medium combinations were, therefore, plotted by a computer.

Based on the 16 stress-strain combinations used here, the average edgewise compressive strength for instance can be predicted from figure 6-a. For the previous 0.0112-0.00854-0.0112-inch A-flute, read the average strength at about 47 lb/in. The effects of increasing each factor 25 percent while holding the others fixed are predicted for the linerboard σ_u in figure 6-c, the linerboard MOE in figure 6-d, the corrugating medium σ_u in figure 6-e, and the corrugating medium MOE in figure 6-f. It is seen by reading along the contours in these figures that the paperboard stress-strain characteristics do indeed have different predicted effects that depend on the linerboard-medium thickness combinations. The reason for this very important in-

Table 3.—Strength prediction of 42-26-42, A-flute, corrugated for various combinations of stress-strain characteristics

Run No.	Linerboard ¹		Corrugating ¹ medium		Edgewise compressive strength <u>Lb/in.</u>	60-inch box top-to-bottom compressive strength <u>Lb</u>
	s _u	MOE	s _u	MOE		
1	-	-	-	-	43.81	780.1
2	+	-	-	-	43.94	781.7
3	-	+	-	-	45.93	856.6
4	+	+	-	-	51.10	927.5
5	-	-	+	-	46.09	810.1
6	+	-	+	-	50.50	867.1
7	-	+	+	-	47.42	877.3
8	+	+	+	-	53.13	954.9
9	-	-	-	+	40.65	746.6
10	+	-	-	+	41.77	757.7
11	-	+	-	+	45.45	854.5
12	+	+	-	+	47.49	882.9
13	-	-	+	+	48.02	840.8
14	+	-	+	+	47.93	839.5
15	-	+	+	+	50.06	918.3
16	+	+	+	+	55.31	989.4
Average Standard deviation					47.41 3.969	855.1 70.37

¹ The +, and - signs designate the high and low values for each factor, as have been established in Factorial Development.

teraction is explained in the section “Relationship Between Mechanism of Failure and Optimum Design” and suggests new criteria for evaluating paperboard.

Box Strength Effects

With a technique to determine the effect of various stress-strain characteristics on edgewise compressive strength it was of interest to see how they would affect box strength. The following is the box compression formula from (7):

$$P = 2.028 P_m^{0.746} (D_x D_y)^{0.127} Z^{0.492} \quad (6)$$

where

- P = box strength (lb),
- P_m = edgewise compressive strength per unit width (lb/in.),
- D_x = flexural stiffness of combined board in machine direction per unit width (lb•in.),
- D_y = flexural stiffness of combined board in cross-machine direction per unit width (lb•in.), and
- Z = box perimeter (in.).

In their calculations, the Institute of Paper Chemistry used empirically derived P_m, D_x, and D_y to make predictions. In this report the predicted edgewise compressive strength and the predicted board stiffness were used. Flexural stiffnesses in both directions were predicted from the calculated moments of inertia for the board times the MOE's of the paperboards as given by the stress-strain relationships. The appendix gives the calculations of the moment of inertia. The board stiffness in the cross-machine direction was derived from the paperboard properties also in that direction. For calculations in the machine direction for this report the paperboard MOE is twice that in the cross-machine direction. This ratio is close to some reported observations (2); its effect is small in eq. (6). Additionally, box strength calculations were performed on a 60-inch perimeter.

Table 3 predicts theoretical container top-to-bottom compressive strengths for 42-26-42 A-Flute related to the stress-strain combinations. The average box strengths and the effects of the paperboard stress-strain characteristics are predicted in figures 7-a through -f for other paperboard thicknesses. The

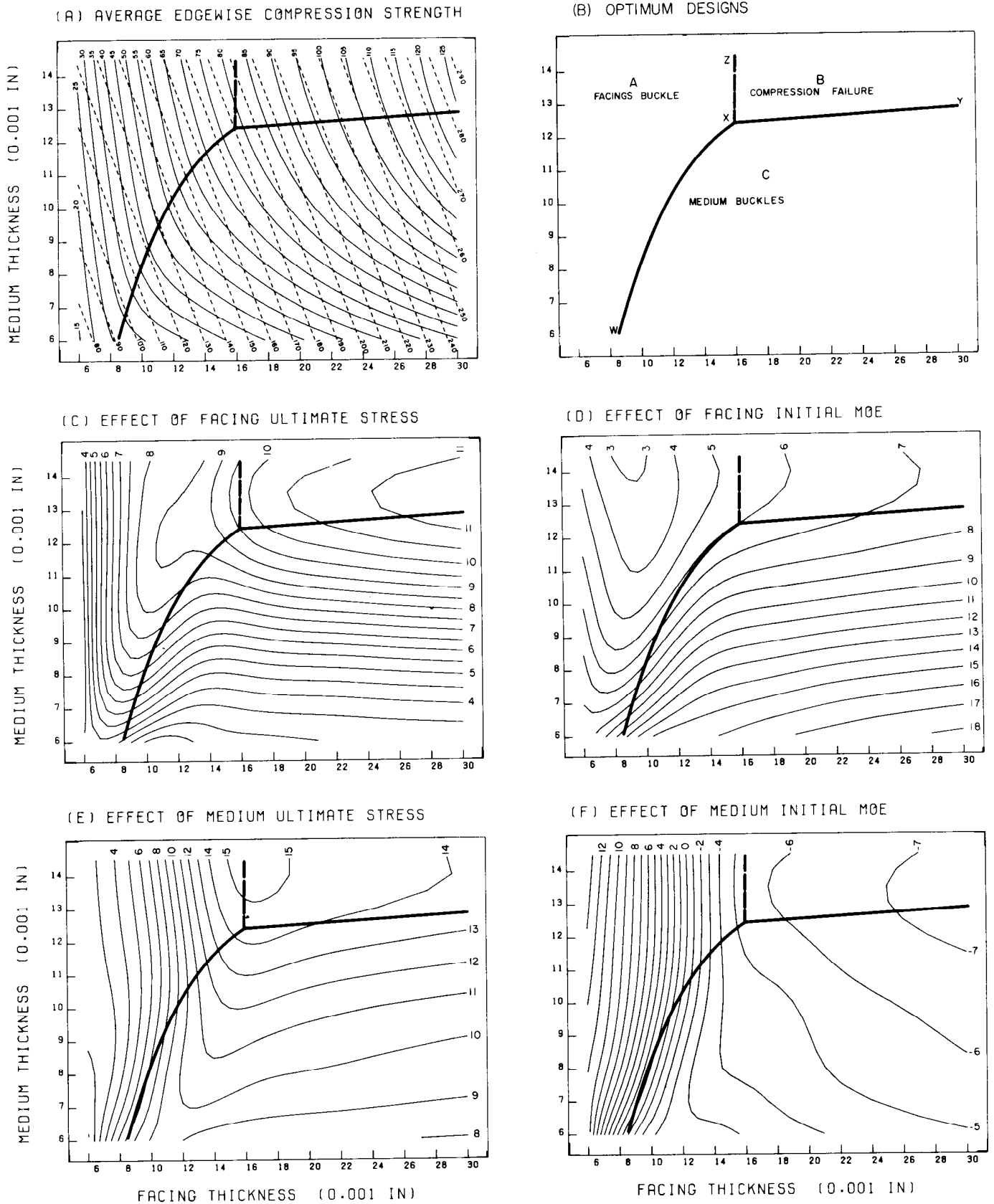


Figure 6.—(a) Average A-flute edgewise compressive strength (lb/in., solid contours) and combined board weight (lb/1,000 ft², dashed contours) for various combinations of facing and medium thickness. (b) The optimum designs and regions of fiberboard failure. (c-f) Contours of effective percent increase in average edgewise compressive strength due to increasing each individual stress-strain characteristic 25 percent and holding all others fixed. (M 148 815)

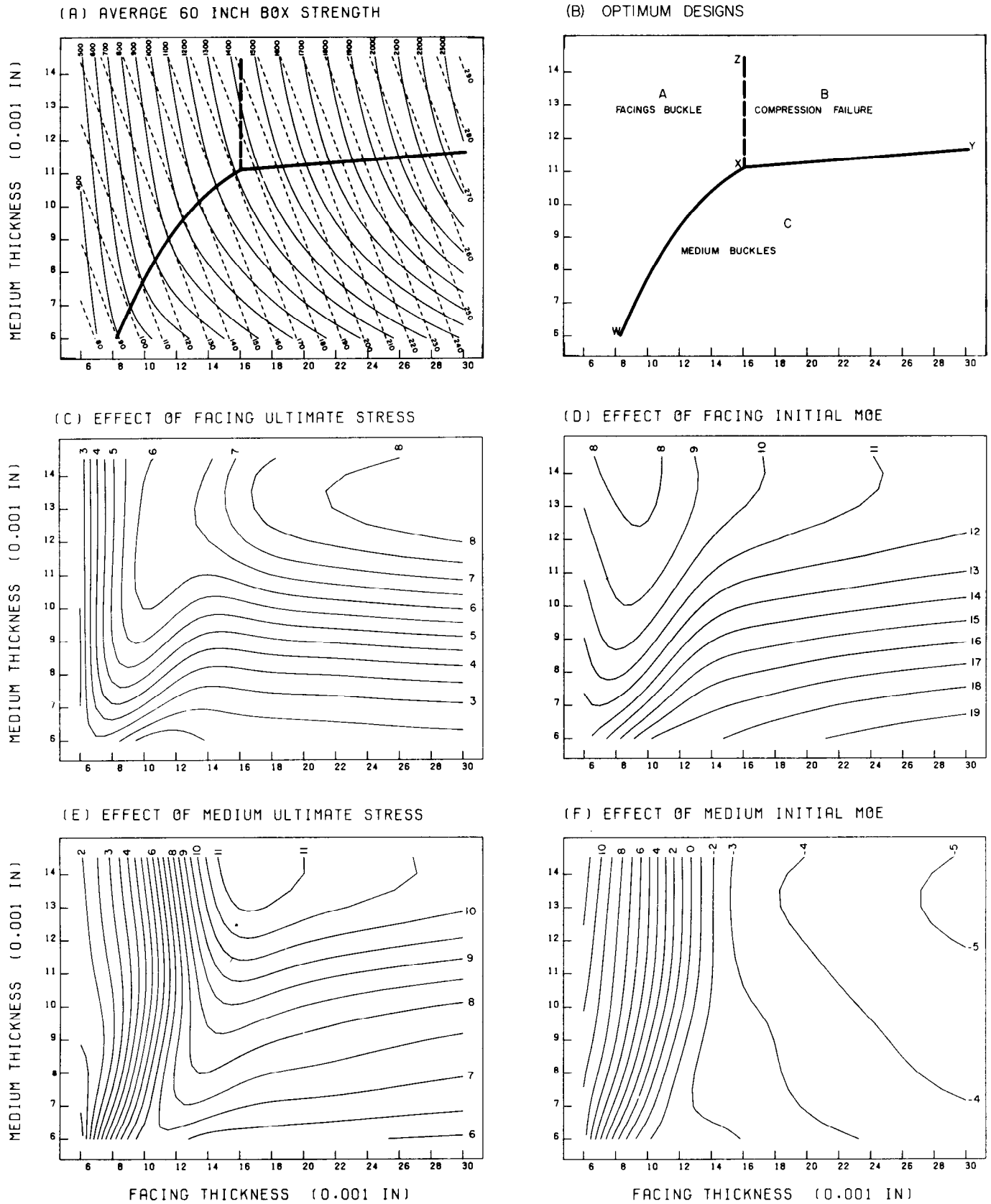


Figure 7.—(a) Average A-flute, 60 inch-perimeter, box top-to-bottom compressive strength (lbs, solid contours) and combined board weight (lbs/1,000 ft², dashed contours) for various combinations of facing and medium thickness. (b) The optimum designs and regions of fiberboard failure. (c-f) Contours of effective percent increase in average box strength due to increasing each individual stress-strain characteristic 25 percent and holding all others fixed.

(M 148 816)

strength for containers with other than 60-inch perimeters can be determined from the following equation:

$$P = 0.1334 P_{60} Z^{0.492} \quad (7)$$

where P_{60} is the box strength read from figure 7-a. The theoretical effects due to the stress-strain characteristics are independent of box perimeter using eq. (6).

Application of Results

Since figures 6 and 7 are based on the results of the

average stress-strain properties of the 16 pairs of curves (fig. 5) it is important to know how to estimate the effects of other pairs of curves. For other stress-strain curves within the range of the experimentally produced curves the corrugated edgewise compressive strength or box strength can be predicted from the linearized factorial model involving only the main effects. In the following expression the subscripts f and m designate the facing or medium characteristic and the effect of some characteristic such as σ_{uf} is denoted by $e(\sigma_{uf})$. This effect is the percentage read from one of the curves (fig. 6 or 7, -c through -f). The strength is thus given by:

$$\text{Strength} = \text{Average strength} \times 1/25 [25 + e(\sigma_{uf})(\sigma_{uf}/1,792 - 1) + e(\text{MOE}_f)(\text{MOE}_f/291,200 - 1) + e(\sigma_{um})(\sigma_{um}/1,432 - 1) + e(\text{MOE}_m)(\text{MOE}_m/290,600 - 1)] \quad (8)$$

Table 4.—Effective percent increase in average strength of A-flute, corrugated due to 25 percent increase in stress-strain characteristic

Main	Stress-strain characteristic ¹	Effective strength increase			
		Edgewise compression		60-inch box top-to-bottom compression	
		0.0112 in facings, 0.00854 in medium	Other combinations	0.0112 in facings, 0.00854 in medium	Other combinations
		<u>Pct</u>	<u>Pct</u>	<u>Pct</u>	<u>Pct</u>
LB	σ_u	6.260	fig. 6-c	4.684	fig. 7-c
LB	MOE	8.749	fig. 6-d	12.30	fig. 7-d
CM	σ_u	10.10	fig. 6-e	7.510	fig. 7-e
CM	MOE	- 1.382	fig. 6-f	- .4338	fig. 7-f
	LB σ_u -LB MOE.	3.322		2.566	
	LB σ_u -CM σ_u	1.798		1.291	
	LB σ_u -CM MOE	- 1.872		- 1.374	
	LB MOE-CM σ_u	- 1.693		- 1.128	
	LB MOE-CM MOE	1.767		1.274	
	CM σ_u -CM MOE	3.586		2.731	
	LB σ_u -LB MOE-CM σ_u	.1793		.1543	
	LB σ_u -LB MOE-CM MOE	.02109		- .06066	
	LB σ_u -CM σ_u -CM MOE	- .7435		- 5267	
	LB MOE-CM σ_u -CM MOE	1.113		.8421	
	LB σ_u -LB MOE-CM σ_u -CM MOE	2.151		1.574	

¹ LB = linerboard, CM = corrugating medium.

Example 1:

Determine the top-to-bottom compressive strength of a 69-33-69 A-flute box with a 45-inch perimeter. The ultimate stress of the linerboard is $\sigma_{uf} = 2,000$, and the initial modulus is $MOE_f = 310,000$. For the corrugating medium the ultimate stress is $\sigma_{um} = 1,500$, and the initial modulus is $MOE_m = 270,000$. The units for these parameters are lb/in.^2 .

Solution:

Use eqs. (4-a,-b) to determine the paperboard thicknesses from the basis weights. The linerboard is 0.0187-inch and the medium is 0.0105-inch-thick. Read from figure 7-a at these thicknesses the average strength of a 60-inch box. $P_{60} = 1,470$ pounds. Determine with eq. (7) the average strength for a perimeter $Z = 45$ inches; average $P = 1,280$ pounds. At the same thicknesses read from figure 7-c the effect of the facing ultimate stress. $e(\sigma_{uf}) = 6.0$. Likewise, read from figure 7-d, $e(MOE_f) = 12.5$; from figure 7-e, $e(\sigma_{um}) = 9.0$; from figure 7-f, $e(MOE_m) = -3.5$. Finally enter all the parameters into eq. (8) to determine the box strength.

$$P = 1,280 \times 1/25 [25 + 6.0 (2,000/1,792 - 1) + 12.5 (310,000/291,200 - 1) + 9.0 (1,500/1,432 - 1) - 3.5 (270,000/290,600 - 1)] = 1,392 \text{ lbs.}$$

Example 2:

A box maker is having difficulty implementing a new tube and cap box made with 69-26-69 A-flute. Reports from the field indicate too-frequent top-to-bottom compression failures. The container supplier says he had improved another customer's box stacking strength at little additional cost by using a stiffer corrugating medium without changing the thickness. That customer was making 38-33-38 A-flute boxes. Determine if the same modification will likewise improve the tube and cap box.

Solution:

The box strength calculations do not apply to the tube and cap design since the formulas are based on experiments on regular slotted containers. However, edgewise compressive strength of the board is highly correlated with box strength. Thus to get a good estimate of the effect of the proposed modification, convert the basis weights to thicknesses using figure 2. Then 69-26-69 is equivalent to 0.0187-0.00854-0.0187 inch and 38-33-38 is equivalent to 0.0100-0.0105-0.0100 inch. Increasing the elastic modulus of the corrugating medium would make it stiffer. Read from figure 6-f the effect on edgewise compressive strength due to increasing the medium initial modulus 25 percent. At the component thicknesses for the 38-33-38 board edgewise compressive strength increases by 5.0 percent. This explains the container supplier's success. However, at the component thicknesses of the tube and cap design, edgewise compressive strength actually decreases by 4.5 percent when the medium elastic modulus is increased. The board strength can be better improved by increasing either the elastic modulus of the linerboard (fig. 6-d) or the ultimate stress of the corrugating

medium (fig. 6-e). The reason for this is explained in the next section.

Relationship Between Mechanism of Failure and Optimum Design

Since it has been shown that the stress-strain characteristics have different predicted effects that depend on the linerboard-medium thickness combination, it is worth investigating by what mechanism the fiberboard structure fails. It is reasonable to believe that the stress-strain characteristics have different effects on the strengths of different board designs because the mechanisms of failure are different. According to the findings in (3) failure in the fiberboard structure can initiate by 1 of 4 mechanisms: buckling in the facings, buckling in the medium, compression in the facings, or compression in the medium.³

The most efficient corrugated design, the optimum design, maximizes strength and is obtained when both components fail simultaneously. Figure 6-a shows the optimum designs for edgewise compressive strength based on the stress-strain curves determined from the experimental data. Contours of constant strength, shown as solid curves, were calculated by the method discussed in "Results of Factorial Analysis." Contours of constant weight, shown as dashed lines give the total board weights based on the paperboard thicknesses, the weight-thickness relationship from eqs. (4-a,-b), and the takeup factor, 1.56. The points at which the strength contours become tangent to the weight contours give the optimum designs. Thus if the facing and medium thicknesses are determined from these points, the edgewise compressive strength of the fiberboard structure is maximized at the minimum weight of combined components.

The optimum designs are plotted in figure 6-a with a thick solid curve, the optimum design plot, which is transposed to figure 6-b, for the purpose of the following discussion, where it separates the linerboard-medium combinations into 3 regions, A, B, and C. Based on the results of (3) the mechanism of failure can be determined within each region as follows: The optimum design plot begins with a positive sloped curve, segment wx, identifying simultaneous buckling failure. If facings and mediums are matched to combinations above or to the left of this curve segment, region A, the fiberboard structure fails by buckling in the facings. If components are matched to combinations below or to the right, region C, the fiberboard fails by buckling in the medium. The plot continues as a nearly horizontal line, segment xy, that separates compression failure, region B, from buckling failure.

³ When a corrugated structure is loaded in edgewise compression parallel to the flutes, failure occurs because (1) the stress in the direction of the load in an element of paperboard between flute tips is below the ultimate stress yet still causes a condition of local instability, i.e., buckling or, (2) the stress equals the ultimate stress for the material, i.e., compression failure.

With a technique for recognizing the mechanism of failure based on the optimum designs, an additional examination of figures 6-a through 6-f will explain how the stress-strain characteristics interact with paperboard thickness and suggest a more effective evaluation of paperboard. First the optimum design plot is superimposed onto figures 6-c through 6-f. Then when the facings and medium are matched to the combinations from region C the fiberboard structure fails by buckling in the medium and an inspection of the lower right corner of each figure, 6-c through 6-f, shows that increasing the initial modulus of the facings most effectively increases edgewise compressive strength. Specifically the numeric values of the contours are maximized in figure 6-d. Thus when the corrugating medium buckles first, increase the linerboard MOE to make it carry more load. When facings and medium are matched to the combinations from region A the fiberboard fails by buckling in the facings and increasing the corrugating medium MOE is most effective. The numeric values of the contours in the upper left corners are maximized in figure 6-f. Thus when the linerboard buckles first, increase the corrugating medium MOE. When the fiberboard fails by compression, region B, increase the corrugating medium σ_u and then the linerboard σ_u .

The preceding generalization is most accurate when the facing-medium combinations are not optimized, i.e., do not intersect the optimum design plot. When they are optimized, the interactions among the stress-strain characteristics become significant. The 0.0112-0.00854-0.0112 inch combination previously discussed and analyzed in tables 3 and 4 is optimized, and a more accurate evaluation of the stress-strain characteristics would require dealing with these interactions.

Example 3:

Explain how the 69-26-69 A-flute structure in example 2 loses strength when the medium stiffness is increased.

Solution:

Since the stress-strain characteristics are not given, use figure 6-a to determine the mechanism of failure based on averages. The 0.0187-0.00854-0.0187-inch design is not optimized and failure occurs at 68 lb/in. by buckling in the medium. Stiffening the medium makes it more able to resist buckling, but also shifts to it some of the compressive load carried by the facings. The benefits derived from a higher buckling strength are offset by the added load it must carry. The net effect is a weaker fiberboard structure.

Estimating the Optimum Design

Because knowing the optimum designs provides a rational evaluation of paperboard in terms of thickness and stress-strain characteristics, it was of interest to obtain the optimum designs for arbitrary stress-strain

properties. The most accurate way of obtaining optimum designs based on the linerboard and corrugating medium stress-strain properties is to plot strength-weight contours like figure 6-a with a computer.

A strength-weight contour plot was produced for edgewise compressive strength and for box strength for each of the stress-strain combinations in table 3. As was previously discussed, the pairs of stress-strain curves used in the calculations were those in figure 5. Space does not permit these 16 edgewise compression and 16 box plots to be reproduced here. In figure 8 only the optimum design plot for each combination determined from the points of tangency between the strength and weight contours is shown.

It is seen that the optimum designs are affected by the stress-strain combinations and that the optimum designs for box strength differ in some cases from those for edgewise compressive strength. It is also seen from runs 9, 13, and 14 that the optimum designs are determined by segment xz in figure 6-b. The reason for this is as follows:

The ultimate strain, ϵ_u , for the paperboard is the strain at the ultimate stress on the stress-strain curve. The ultimate strain for the combined board, ϵ_{ub} , is the lesser of the ϵ_u 's for the linerboard and medium. According to the stress-strain relationship for each

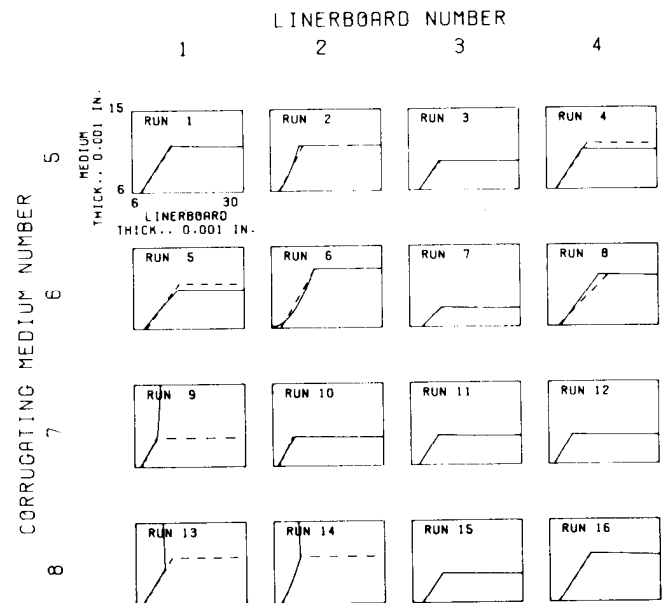


Figure 8.—Optimum design plots for A-flute edgewise compressive strength (solid curve) and for box top-to-bottom compressive strength (dashed curve). The linerboard and corrugating medium stress-strain relationships are given in figure 5.

(M 148 819)

component in the form of eq. (1), if $\sigma(\epsilon_{ub})$ for the fixings is greater [less]⁴ than $\sigma(\epsilon_{ub})$ for the medium, the line is horizontal [vertical]. Above [to the right of] this line the structure fails by compression in the component with the lower ϵ_u .

To relate paperboard characteristics with arbitrary stress-strain curves within the range of the experimentally produced curves to box compressive strength, the following method can be used to estimate the optimum designs: First, segment wx of the optimum design plots that identify simultaneous buckling failure have only marginal differences resulting from the different stress-strain combinations. The use of figure 7-b⁵ to separate facing from medium buckling based on averages is therefore accurate for the data in this report. Next, segment xy of the box optimum design plot separates medium buckling from compression failure and an average segment can be determined from figure 7-b. However, this segment can be more accurately determined for other stress-strain curves if the component stress-strain relationships are given in the form of eq. (1).

At ϵ_{ub} determine the stress in the corrugating medium σ_m , where $\sigma_m = \sigma(\epsilon_{ub})$. Next, solve eq. (2-a) to determine the slope of the stress-strain curve for each component at ϵ_{ub} denoted by the tangent modulus E_t , where $E_t = \sigma'(\epsilon_{ub})$. The separation between compression failure and medium buckling occurs at the medium thickness

$$t_m \text{ (in.)} = 0.0107 - 6.02 \cdot 10^{-13} E_{tf} \cdot E_{tm} \text{ (lb}^2/\text{in.}^4) \\ + 3.22 \cdot 10^{-11} E_{tf} \cdot \sigma_m \text{ (lb}^2/\text{in.}^4)$$

where the subscripts f or m denote the facing or medium component.

Conclusions

Corrugated fiberboard is made up of interconnecting linerboard and medium plates (fig. 1) whose dimensions are determined by the flute profile. The theoretical effects of the paperboard stress-strain characteristics depend on the linerboard and corrugating medium thicknesses. For example, from figure 6-d, increasing the linerboard modulus of elasticity 25 percent and holding all other stress-strain characteristics fixed results in an edgewise compressive strength increase of about 13.5 percent for 90-26-90 A-flute (i.e., 0.0246-0.00854-0.0246 inch), but only 5 percent for 38-33-38 A-flute (i.e., 0.0100-0.0105-0.0100 inch).

To what degree the stress-strain characteristics affect corrugated strength can be explained by the optimum designs. From figure 6-b, 90-26-90 A-flute fails by buckling in the corrugating medium and 38-33-38 A-flute, by

buckling in the facings. When the medium buckles prematurely the facing elastic modulus should be increased, rather than the medium's. This is because the linerboard and medium jointly share the axially applied load proportioned according to their individual paperboard moduli times their cross sectional areas. Increasing the modulus of the stronger component (in this case, the facings) will accordingly force it to carry more of the load.

The same conclusion is drawn from studying the effect of increasing the medium modulus of elasticity. For 38-33-38 A-flute edgewise compressive strength increases (fig. 6-f) by 5 percent, but for 90-26-90 A-flute, it decreases by 5.5 percent. When buckling initiates in the facings, increase the medium elastic modulus. For an efficient design one should therefore add thickness to the weaker component to approach the optimum design and add stiffness to the stronger component.

When failure occurs by compression, corrugated strength is most improved by increasing the ultimate stress of either component. The thickness of the medium which governs the transition between medium buckling and compression failure can be determined from the component stress-strain properties.

Further research is being conducted to check the accuracy of these conclusions.

Literature Cited

1. Baum, G. A., and C. C. Habeger.
1980. On-line measurement of paper mechanical properties. Tappi Vol. 63, No. 7. July.
2. Jackson, C. A., J. W. Koning, and W. A. Gatz.
1976. Edgewise compressive test of paperboard by a new method. Pulp and Paper Canada Vol. 77, No. 10. Oct.
3. Johnson, M. W., Jr., T. J. Urbanik, and W. E. Denniston
1979. Optimum fiber distribution in singlewall corrugated fiberboard. USDA, For. Serv. Res. Pap. FPL 348.
4. Koning, J. W., Jr.
1975. Compressive properties of linerboard as related to corrugated fiberboard containers: A theoretical model. Tappi Vol. 58, No. 12. Dec.
5. Koning, J. W., Jr.
1978. Compression properties of linerboard as related to corrugated fiberboard containers. Theoretical model verification. Tappi Vol. 61, No. 8. Aug.

⁴ Text in brackets gives the alternate occurrence.

⁵ Figure 7-b was determined from figure 7-a based on the method discussed in the previous section.

6. Koning, J. W., Jr., and J. H. Haskell.
1979. Papermaking factors that influence the strength of linerboard weight handsheets. USDA, For. Serv. Res. Pap. FPL 323.
7. McKee, R. C., J. W. Gander, and J. R. Wachuta.
1963. Compression strength formula for corrugated boxes. Paperboard Packaging Rep. 79. Sept. 10.
6. Moody, R. C.
1965. Edgewise compression strength of corrugated fiberboard as determined by local instability. USDA, For. Serv. Res. Pap. FPL 46.
9. Page, D. H., R. S. Seth, and J. H. DeGrace.
1979. The elastic modulus of paper. I. The controlling mechanisms. Tappi Vol. 62, No. 9. Sept.
10. Setterholm, V. C.
1974. A new concept in paper thickness measurement. Tappi Vol. 57, No. 3. Mar.
11. Takahashi, H., and H. Suzuki.
1979. The effect of fiber shape on the mechanical strength of paper and board. Tappi Vol. 62, No. 7. July.
12. University of Wisconsin.
1972. Nonlinear Regression Routines. Academic Computing Center, Madison.

Appendix

The structural cross sectional geometry is shown in figure 1. The flute profile determines the flute height h_f , flute pitch p , and takeup factor TF. From these parameters, the facing thickness t_f and medium thickness t_m calculate the individual member widths.

$$a_1 = \frac{p^2 (TF^2 - 1) - 4 (h_f - t_m)^2}{4 p (TF - 1)}$$

$$a_2 = p - a_1$$

$$a_3 = p TF/2 - a_1$$

Next determine the angle α .

$$\alpha = \tan^{-1} \frac{h_f - t_m}{(p/2 - a_1)}$$

The moments of inertia about the neutral axis of the board per unit board width become for each member:

$$I_1 = a_1/p (t_m^3/6 + t_m(h_f - t_m)^2/2)$$

$$I_2 = t_f^3/6 + t_f(h_f + t_f)^2/2$$

$$I_3 = (t_m a_3^3 + a_3 t_m^3 + (a_3 t_m^3 - t_m a_3^3) \cos(2\alpha))/12 p$$

Then the moments of inertia per unit board width in each direction are determined from the individual member contributions. In the machine direction:

$$I_{md} = I_2$$

In the cross-machine direction:

$$I_{cmd} = I_1 + I_2 + I_3$$